

Motivation

Surface mass variations from hydrological, oceanic, and atmospheric processes deform the lithosphere and may modulate seismicity. This study examines subduction zones to assess how such loading influences the stress status and earthquake potential.

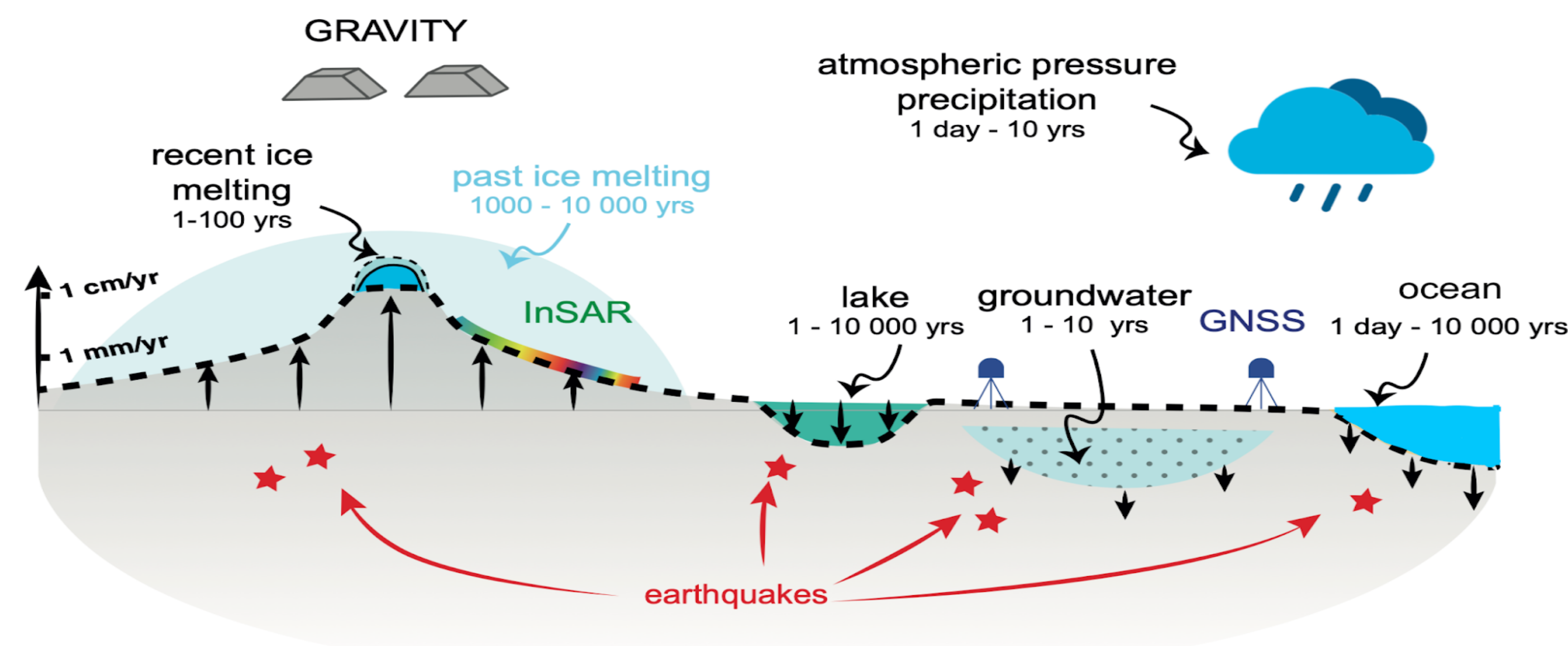


Fig.1. Sketch of (visco-) elastic climate-driven loading. Modified from fig 1 in Bürgmann, R., et.al. 2024.

Approach 1: multi-loading-induced Δ CFF, regional (Kuril-Japan)

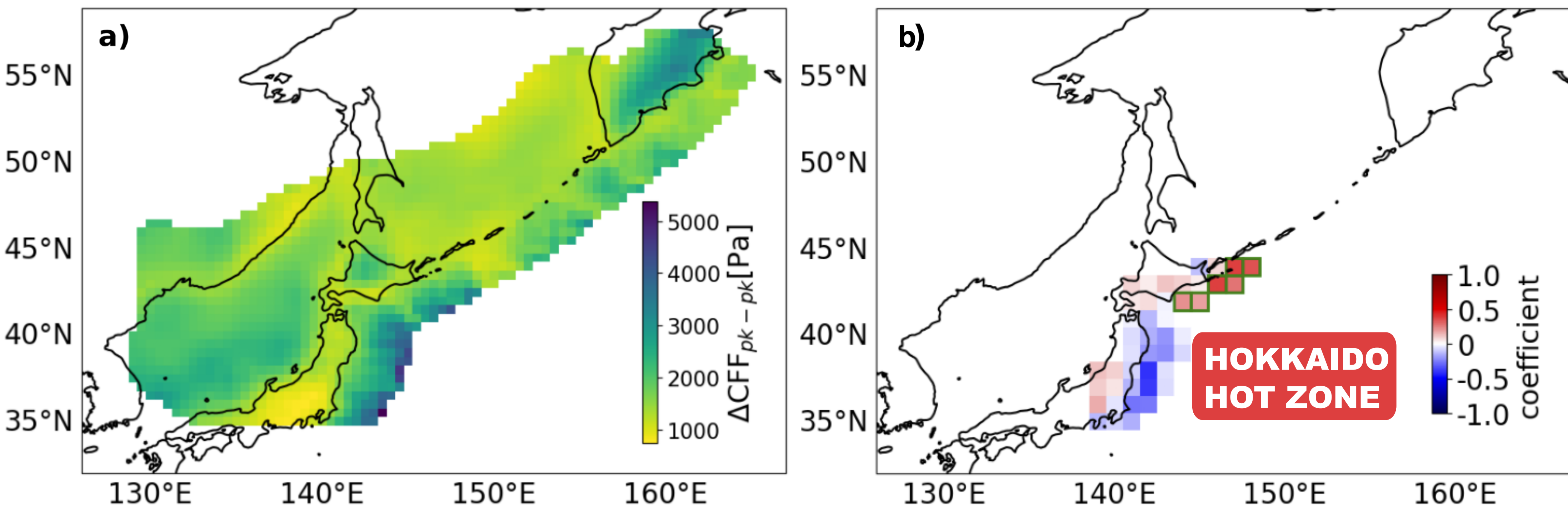
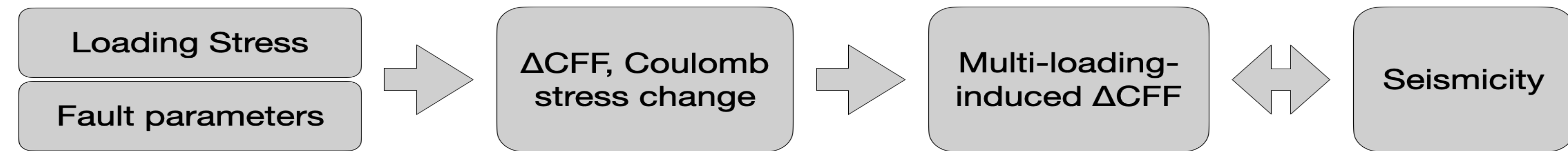


Fig.2. a) The peak-to-peak amplitudes of the depth-dependent Δ CFF. The shallow edge of the Japan Trench experiences the lowest amplitude at 0.8 kPa. The slab beneath the Kamchatka Peninsula experiences the highest amplitude, reaching about 4 kPa. b) Correlation coefficients between multiple surface-loading-induced Coulomb stress change Δ CFF and excess (or deficiency) earthquake rate R_{ex} . Hokkaido Hot Zone patches with a statistically significant positive correlation are highlighted with green bounding boxes.

1. Statistically significant positive correlation is observed.

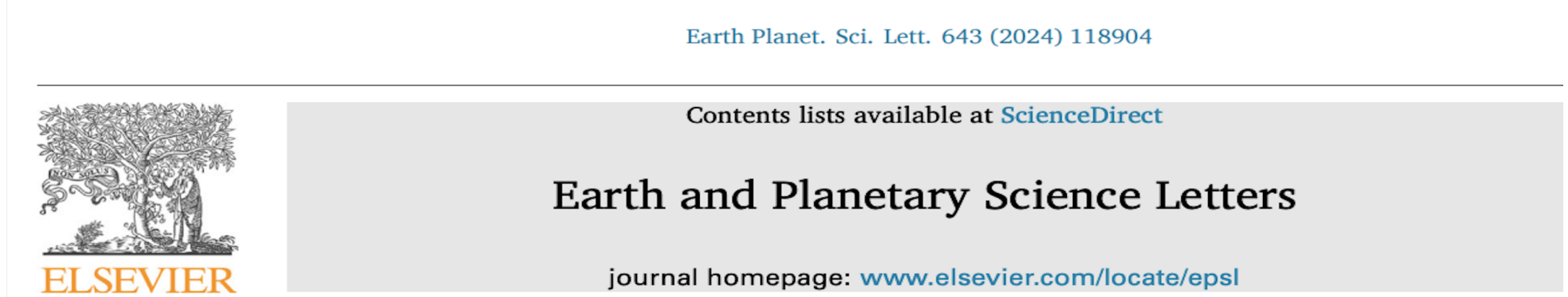
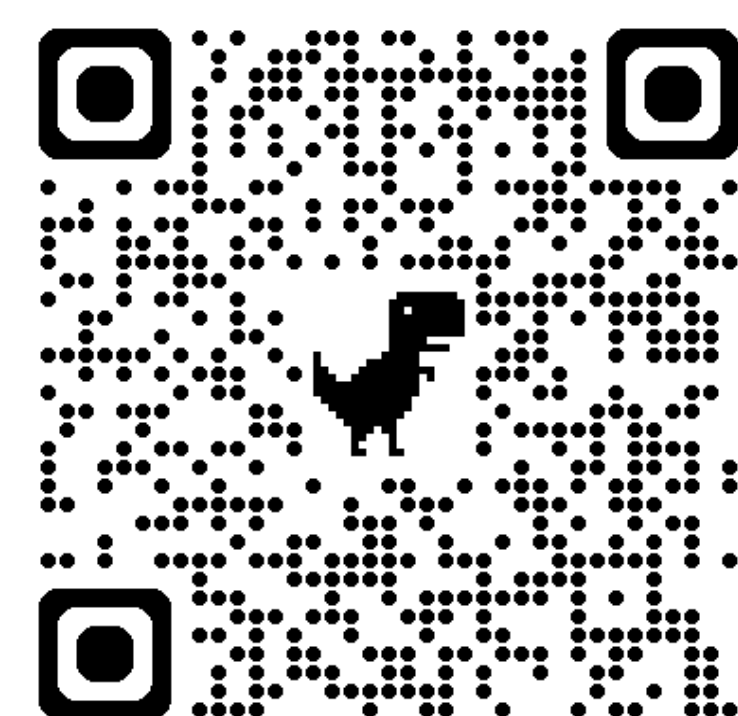
2. Primary loading source varies across regions.

3. Cumulative impact matters!

TAKEAWAYS

Further reading

Cai, Y., & Mouyen, M. (2024). Loading-induced stress variation on active faults and seismicity modulation in the Kuril Islands-Japan region. *Earth and Planetary Science Letters*, 643, 118904.



Loading-induced stress variation on active faults and seismicity modulation in the Kuril Islands-Japan region
Yiting Cai *, Maxime Mouyen

Surface Loading and Seismicity in Subduction Zones: Linking Stress Changes to Fault Failure

Yiting Cai ¹, Roland Bürgmann ²

1. Department of Space, Earth, and Environment, Chalmers University of Technology, Gothenburg, Sweden, yiting.cai@chalmers.se
2. Department of Earth and Planetary Science, University of California, Berkeley, Berkeley, CA, USA, burgmann@berkeley.edu

Approach 2: multi-loading-induced $\Delta\sigma$, global subduction zones

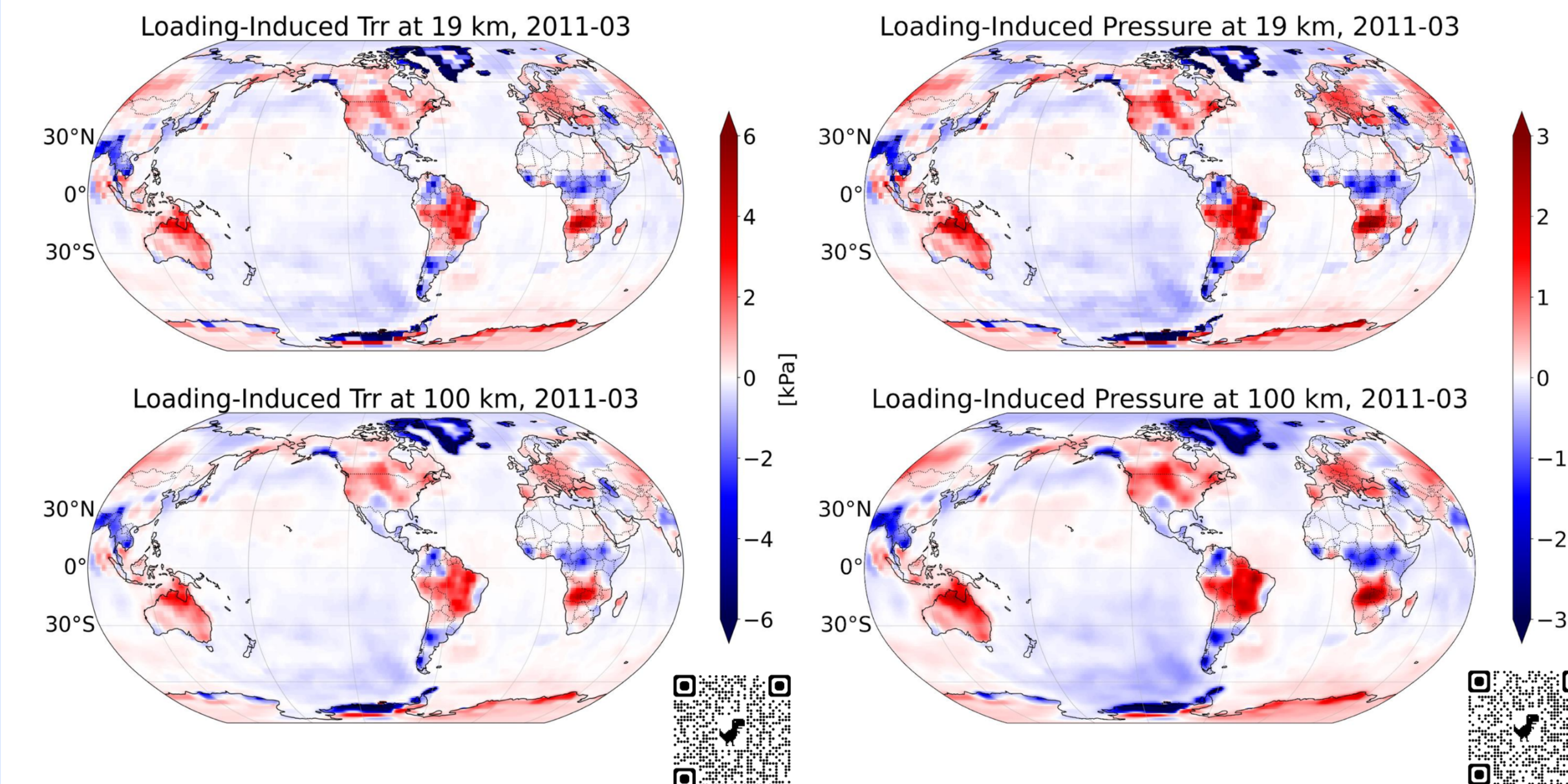
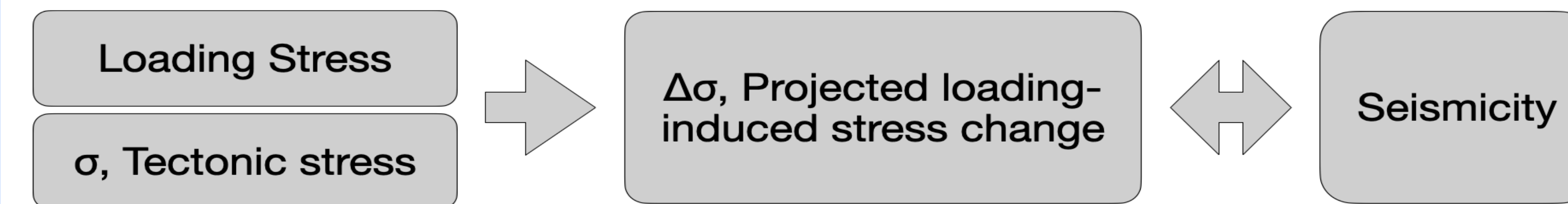


Fig.3. Vertical stress (left) and the volumetric stress (right) variations due to the global surface loadings, computed from the GRACE/GRACE-FO JPL MASCON RL06 product, including continental water, ocean water, and the atmospheric pressure. Positive values represents compression. Please scan the QR code for videos between 2002-2021.

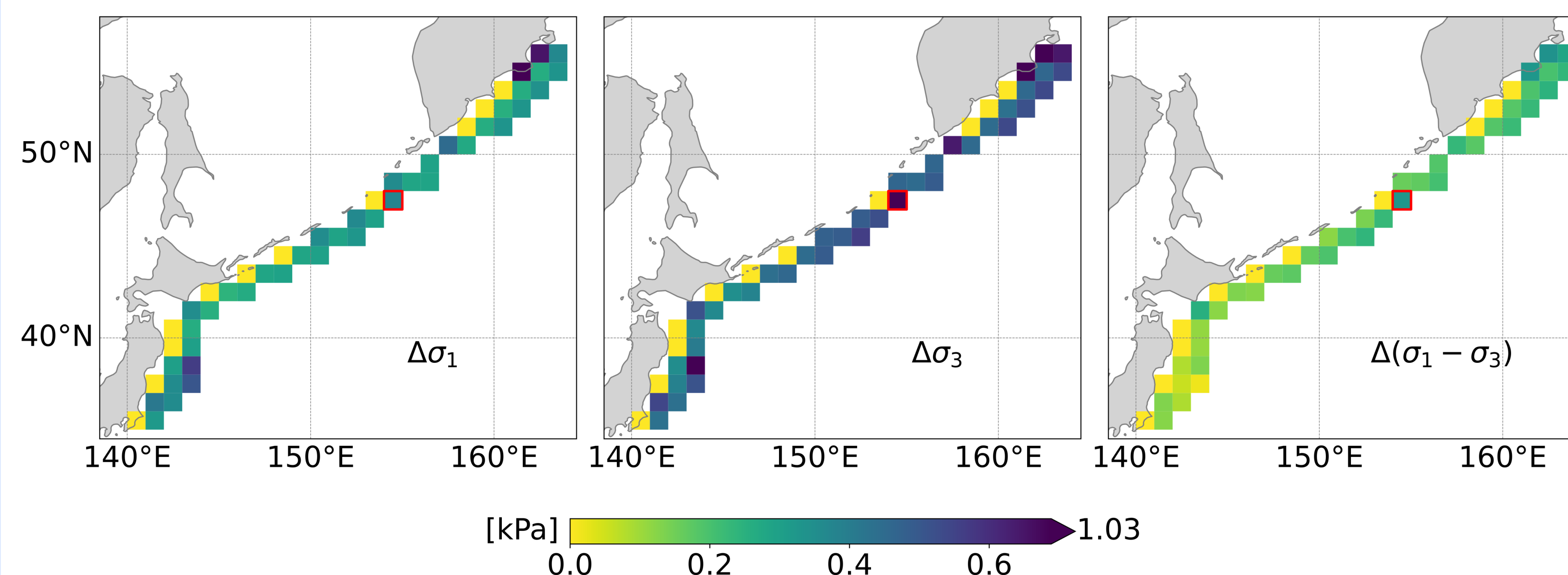


Fig.5. Map of annual peak-to-peak amplitudes of loading-induced stress change projected in the σ_1 , σ_3 orientation, and the differential stress ($\sigma_1 - \sigma_3$) for Kuril Megathrust.

Ongoing work: $\Delta\sigma$ v.s. seismicity

Long-term background tectonic stress orientation, derived from ~35k subduction zone earthquakes in the GCMT catalog (1976–2024), is used together with seasonally varying stress tensor time series to assess changes relative to the background stress principal axes.

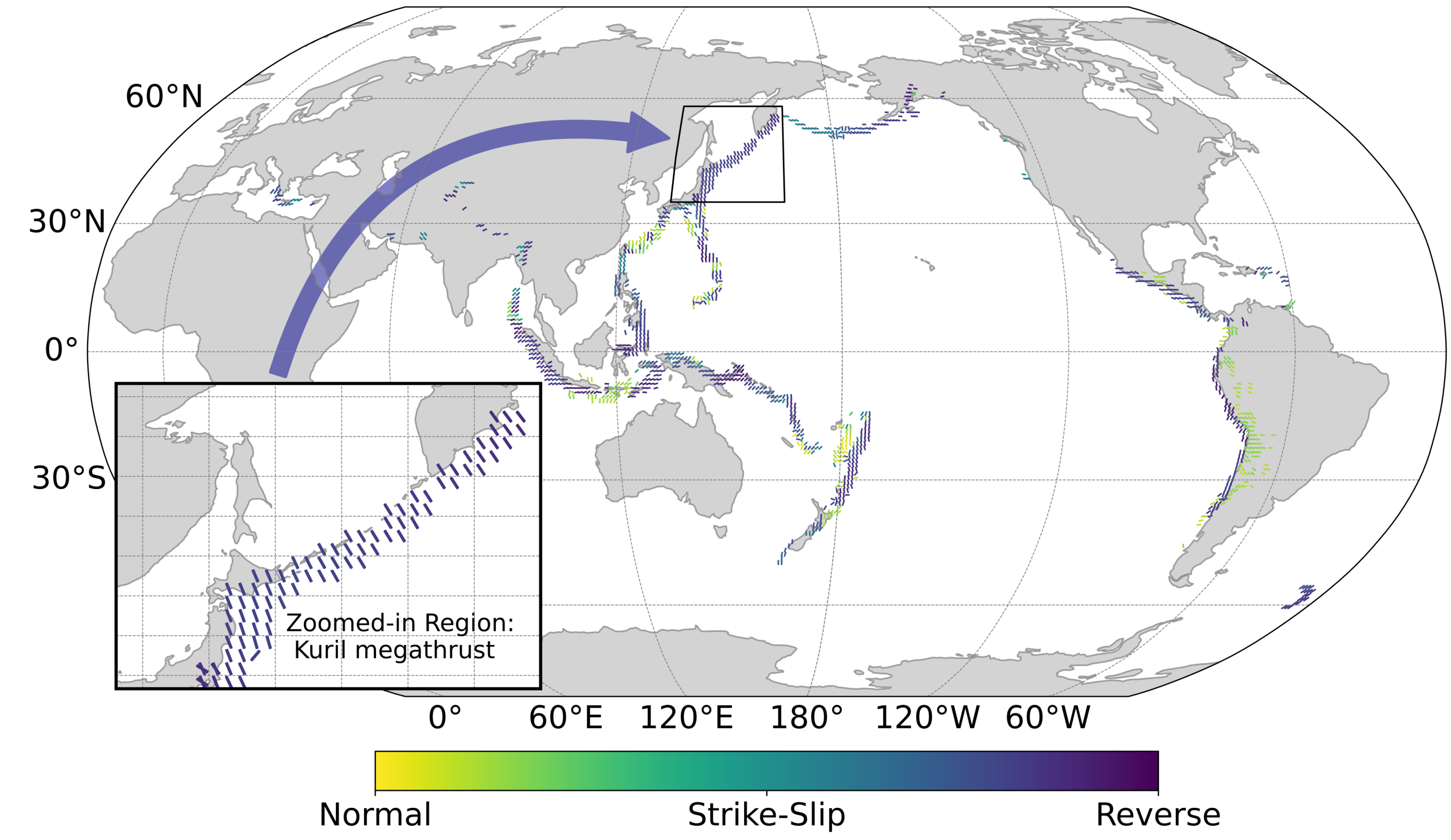


Fig.4. Background stress field (maximum horizontal compressional stress direction) for the major subduction zones given in Slab2 model, Hayes, G.P. et. al. 2018. The faulting style follows the Simpson's convention.

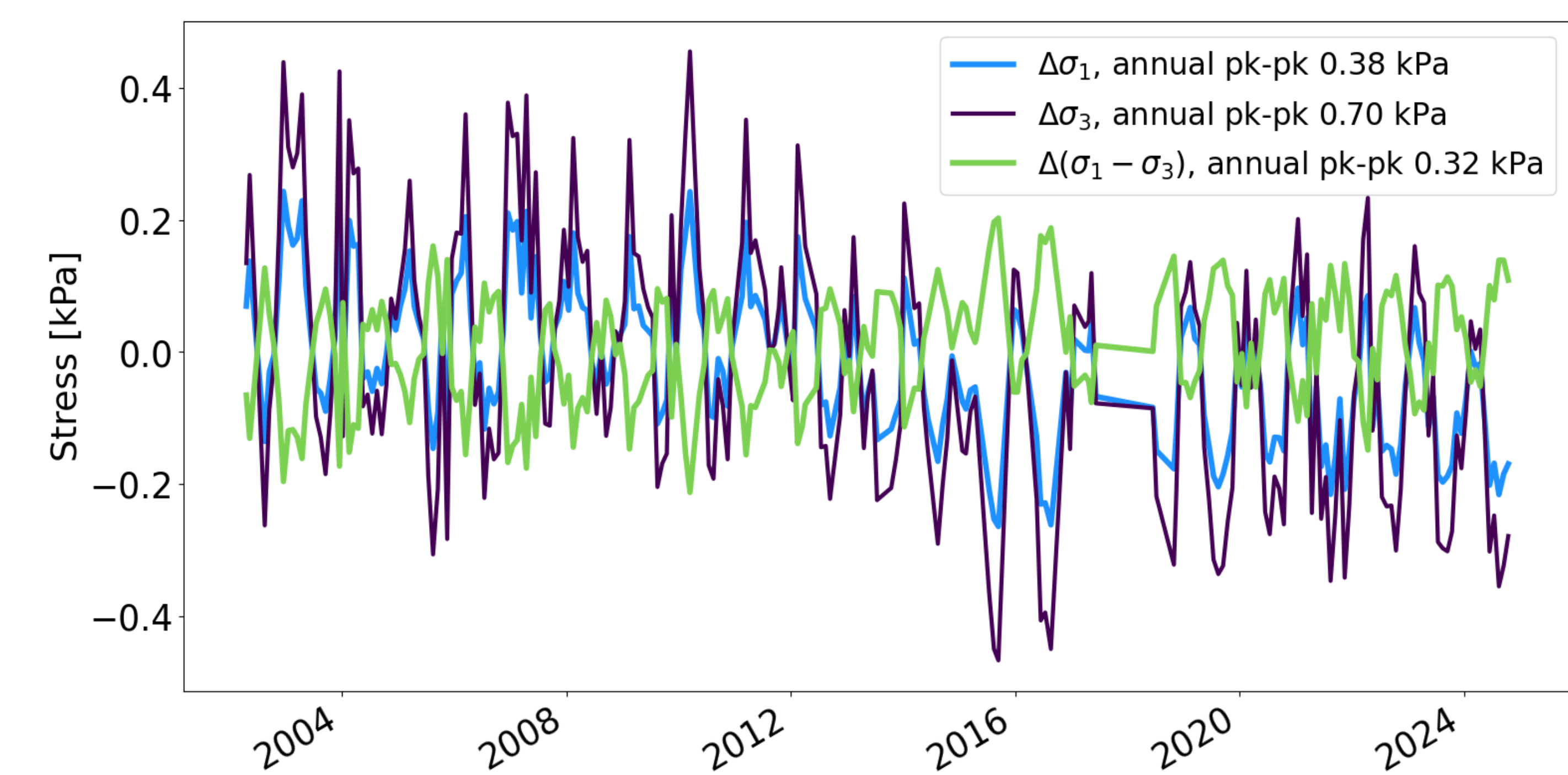


Fig. 6. Loading-induced stress changes projected in the σ_1 , σ_3 orientation, and the differential stress ($\sigma_1 - \sigma_3$), for a 1-degree patch centered at 154.5°E, 47.5°N of Kuril megathrust, highlighted with red boxes in Fig.5.



Poster QR



Acknowledgments

The computations and data handling were enabled by resources provided by the National Facility Computing Infrastructure (NFCI) at Onsala Space Observatory, Chalmers e-Commons at Chalmers, and the National Academic Infrastructure for Supercomputing in Sweden (NAISS), partially funded by the Swedish Research Council through grant agreement no. 2022-06725.

Participation of EGU25 is funded by SSA Global Travel Grant.

